PROPERTIES OF MARTENSITIC STAINLESS STEEL BEFORE AND AFTER CYCLIC LOADING

KUČERA Pavel[1], MAZANCOVÁ Eva[2]

[1]*VÍTKOVICE CYLINDERS Inc., Ostrava, Czech Republic, EU, pavel.kucera.@vitkovice.cz*
[2]*VSB - Technical University of Ostrava, Faculty of metallurgy and materials Engineering, Ostrava, Czech Republic, EU, eva.mazancova@vsb.cz*

Abstract

Paper deals with the martensitic stainless steel (MSS) after reversed extrusion and broaching, quenching into polymer from austenitization temperature of 1130 °C and subsequently tempered at 480 °C with final cooling in the air. Wall thickness of cylinders corresponded to 5 mm. Subsequently some cylinders were cyclically loaded. Basic mechanical properties and microstructure features together with fracture analysis of cylinders before and after cyclic loading were compared.

Keywords: Martensitic stainless steel, mechanical properties, fracture analysis, cyclic loading, microstructure

1. INTRODUCTION

The cyclic response is one of the crucial design properties of all mechanically or pressure loaded components. Since all materials change their mechanical properties during the cycle loading (e.g. cyclic hardening and cyclic softening), it is very important to understand those changes for each steel type. High strength (1000 MPa +) martensitic stainless steels (SS) are commonly used in variety of applications, such as highly loaded flanges for oil and natural gas mining and transport, high pressure hydraulic components in environment with high salinity and newly also high pressure steel cylinders (HPSC) manufacturing for storage and transport of natural gas, corrosive gases, scuba diving and highly pure gases. Such material has to withstand quiet severe testing conditions as it is presented in [1] to prove its significant corrosion resistance to variety of environments. This type of steels is also well resistant to hydrogen embrittlement as [2 - 4] are presenting. There is an extensive world-wide work done to increase mechanical, corrosion, fracture and other properties and such work is represented by work of Foroozemehr [5] and Ma [6, 7] and Ye [8]. However evidence of the cycle life of such material type is known, but only in case of single or bi-axial loading. Some of applications, such as pipes, flanges, pressure components are intended to be used in tri-axial loading same as high pressure steel cylinders. To simulate such loading, the special equipment is needed to achieve tri-axial loading. This is achievable only by the internal over pressurization by fluid to simulate as closest condition as possible to real cyclic pressurization during the real process. Intention of this paper is to evaluate the influence of tri-axial cycle loading on the high pressure cylinder (tubes) made of martensitic SS and to estimate what processes take place during with certain results. The investigation in this paper was based on the seven steps - chemical composition and mechanical properties testing, cycle loading microstructural, mechanical testing after cycle loading, micro purity with grainsize and fracture analysis. Results of mentioned investigation are evaluated and compared with the cylinders made of steel AISI 4135, which is used as common material for HPSC manufacturing.

2. EXPERIMENTAL PROCESSES AND RESULTS

The experimental examination began with the analysis of chemical composition of martensitic SS input material - hot forged bar is following [in wt. %]: 0.05 C, 0.69 Si, 0.46 Mn, 14.99 Cr, 3.97 Ni, 0.79 Mo, 0.019

N, 0.011 S and 0.039 P. AISI 4135 steel chemical composition revealed following values: 0.38 C, 0.33 Si, 0.71 Mn, 1.12 Cr, 0.024 Ni, 0.23 Mo, 0.004 S and 0.009 P.

Second step was based on the forming processes of input billet - reverse extrusion and broaching, subsequently neck forming and finally the heat treatment based on the austenitization at 1130 °C together with the tempering at 480 °C with subsequent air cooling were carried out. After all mentioned processes second chemical analysis of final product was carried out to evaluate the redistribution of certain chemical elements with final results in case of SS are [in wt. %]: 0.04 C, 0.73 Si, 0.41 Mn, 14.87 Cr, 3.93 Ni, 0.76 Mo, 0.020 N, 0.013 S and 0.036 P. Same processes were applied in case of AISI 4135 however the austenitization temperature was set to 890 °C with subsequent quenching and tempering with resulting chemical composition was [in wt. %]: 0.36 C, 0.67 Si, 0.42 Mn, 1.10 Cr, 0.021 Ni, 0.22 Mo, 0.012 S and 0.038 P.

Table 1 Mechanical properties after HT (average values from 2 samples)

Spec.	YS [MPa]	TS [MPa]	El. [%]	CVN $_{transverse\ -50\ °C}$ [J / cm^{-2}]	CVN $_{longitudinal-50\ °C}$ [J / cm^{-2}]	HBW (2.5 / 187.5) [-]
MSS	900	1023	18.6	125	110	315
AISI 4135	957	1022	16	75	90	310

One cylinder of each material after the heat treatment was used for the test samples extraction and the mechanical properties testing was the third step of an experimental processes and was focused on the testing of yield strength (YS), tensile strength (TS), elongation (El.), CVN and Brinell hardness (HBW). To test the tensile properties the Zwick / Roell Z 250 machine was used according to the EN ISO 6892-1. The hardness testing machine M4U750 was used to measure achieved hardness according to the EN ISO 6506-1. Notch toughness testing was carried out using RKP 450 Charpy Impact Testing Machine according to the ISO 148-1 at -50 °C in transverse and longitudinal direction. Mechanical properties results are summarized in **Table 1.**

The next, fourth step of investigation was cycle loading according to ISO 9808-1 standard. Two cylinders of each material after heat treatment were cycle loaded with the setup of lower internal pressure to 30 bar and the (upper) test pressure was set to 345 bar with the frequency of 0,25 Hz. Results of cycle loading of AISI 4135 and martensitic SS to the fracture are listed in **Table 2**. **Table 3** summarizes results of mechanical testing after cycle loading.

Table 2 Results of cycle loading

Sample number	Number of achieved cycles
1 (AISI 4135)	29899
2 (AISI 4135)	31945
3 (Martensitic stainless steel)	80945
4 (Martensitic stainless steel)	84376

Table 3 Mechanical properties after cycle loading (average values from 2 samples)

Spec.	YS [MPa]	TS [MPa]	El. [%]	CVN $_{transverse\ -50\ °C}$ [J / cm^{-2}]	CVN $_{longitudinal-50\ °C}$ [J / cm^{-2}]	HBW (2.5 / 187.5) [-]
MSS	902	1009	23.6	146	134	315
AISI 4135	972	1065	17.7	73	86	323

Metallographic observation was focused on microstructure after the heat treatment, micro-purity and grain size evaluation using the light microscopy (Olympus IX70). For micro-fractography investigation was the SEM

(scanning electron microscopy SEM JEOL JSM-6490 LV equipped with X-ray analyser EDA) used. Metallographic samples of the finished cylinder from each material were prepared in transverse direction by the grinding; polishing and etching in Nital and/or in sodium hydroxide. **Figure 1** is revealing the tempered martensite microstructure with the presence of approximately between 8 and 10 wt. % of δ-ferrite. In the **Figure 2**, the presence of tempered martensite together with the presence of segregation bands is visible.

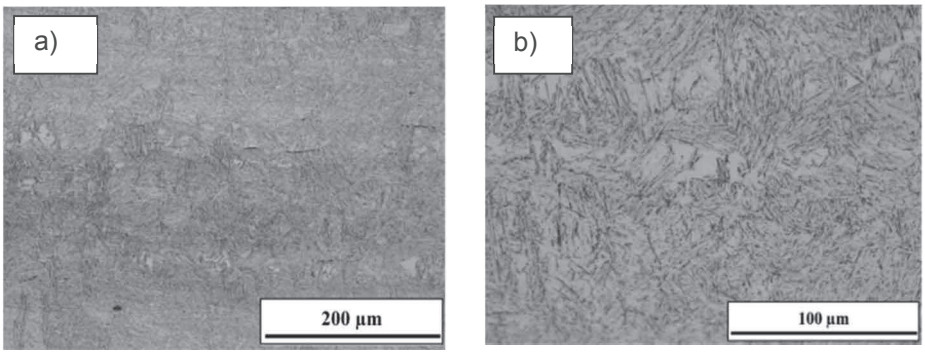

Figure 1 δ-ferrite in tempered martensite (martensitic stainless steel) in central area of wall thickness (transversal direction) a) general view, b) in detail

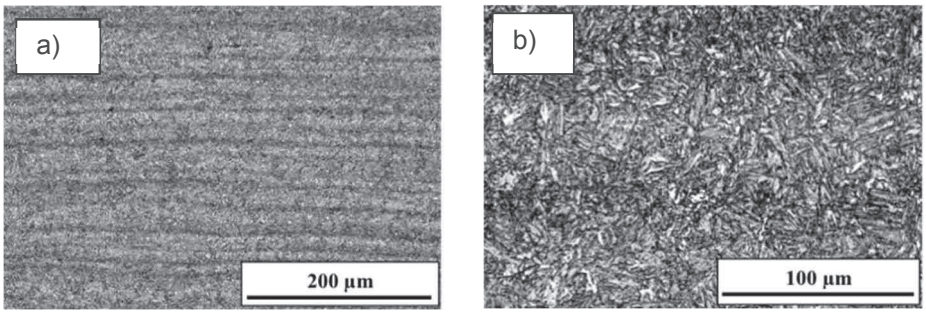

Figure 2 Tempered martensite with segregation bands (AISI 4135) a) general view, b) in detail

Table 4 Evaluation of micro purity and grain size of final products

Material	Sulphides fine/coarse	Oxides banded fine/coarse	Oxides formable fine/coarse	Globular oxides fine/coarse	Coarse globular oxides fine/coarse	Grain size
MSS	-	0.2 / 0.1	0.1 / 0.3	0.4 / 0.1	0.2	9
AISI 4135	-	0.3/-	0.2/0.1	0.3/0.2	0.1	10

Grain size of finished cylinders according to EN ISO643 and micro purity according to ISO 4967 evaluation are shown in **Table 4.**

The SEM analysis of martensitic SS revealed the presence of crack morphology typical for fatigue loading. Crack initiated from the internal surface on the rougher inequality, scratch or possibly oxidized surface, see **Figure 3(1)**. The presence of non-metallic inclusions such as sulphides was found as it can be seen in **Figure 3(2)**. Further crack propagation caused the combination of transcrystalline cleavage and also interkrystalline fracture morphology as it is documented in **Figure 3(3)**. **Figure 3(4)** and **3(5)** show the presence of minor micro-cracks presence. And as the last stage of the crack propagation, beach marks presence in **Figure 3(6)** is documented and subsequently extensive beach marks with final crack stage (non-stable crack propagation) of material together with the one of final crack is shown in **Figure 3(7).**

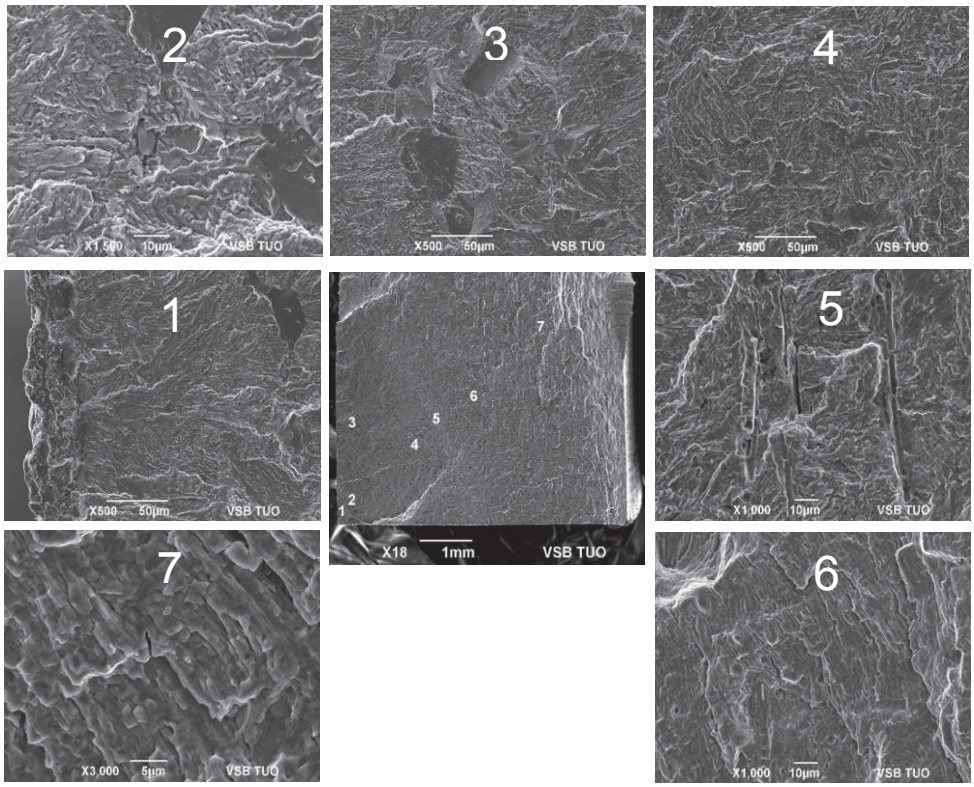

Figure 3 Fracture surface of MSS after cycle loading

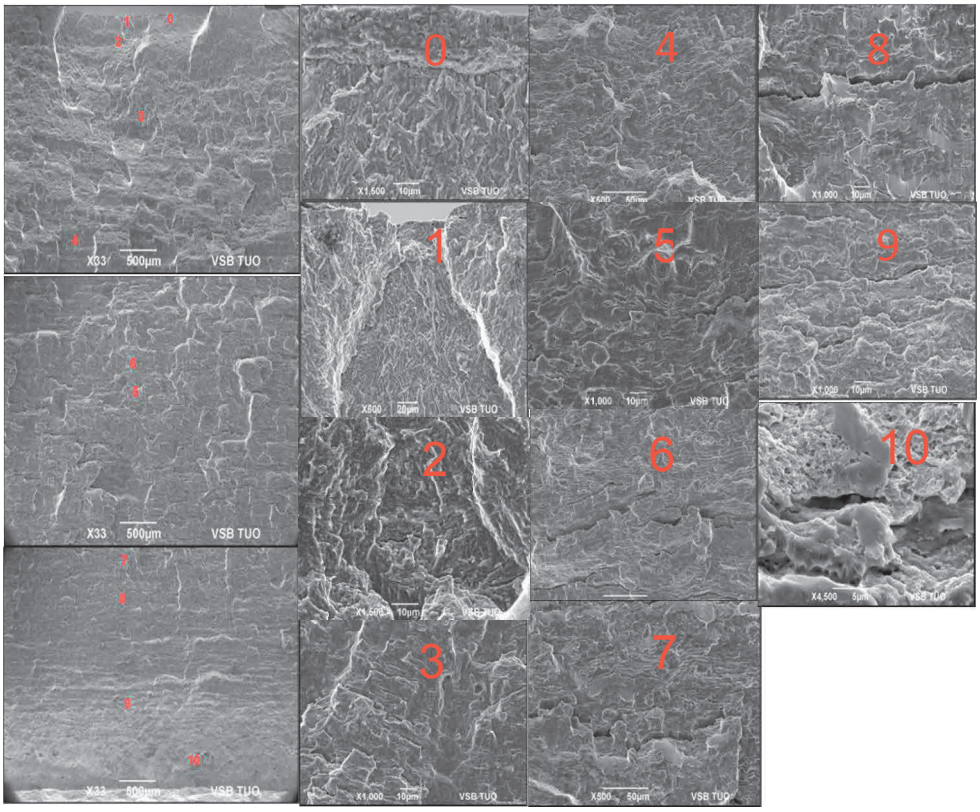

Figure 4 Fracture surface of AISI 4135 steel after cycle loading

Scanning electron microscopy analysis carried out on the 34CrMo4 steel revealed also the typical fracture morphology for standard fatigue process. **Figure 4(0)** presents the crack initiation area probably caused by the locally decarburized area since the layer of scales is clearly visible. The crack propagation area is documented in **Figure 4(1)**. Further continuous cycle loading caused the crack propagation in form of mainly transcrystalline cleavage fracture as **Figure 4(2)** shows. There is a visible beach marks initial presence showed on **Figure 4(3)** and is continuing to **Figure 4(6)** where is the area of larger connecting cracks presence with subsequent non-stable crack propagation as it is shown in **Figures 4(7) - 4(9). Figure 4(10)** revealed the final crack area with a combination of trancrystalline cleavage fracture and ductile fracture with visible dimples.

3. DISCUSSION

As **Table 3** shows, two different types of steel, however with very similar microstructure as it is presented in **Figures 1** and **2** and corresponds with [9 and 10] revealed significantly different behaviour after cycle loading. Martensitic SS experiences the cyclic softening with the lowered TS by 14 MPa and considerable increased El. by 5 % together with also major increase of CVN values. Martensitic SS generally show great fatigue response in all fields as it is presented in [11] and directly corresponds with achieved results of cycle number that are 2.7 times higher in case of MSS compared to the ASI 4135 steel. It can be estimated that the presence of larger amount of δ-ferrite, which will occur in steel always in some certain amount as it is presented in [12], does not affect achieved favourable results of mechanical properties in contrary with work of Wang [13] In case of AISI 4135 mechanical testing results after cycle loading (see **Table 2**) was found a significant cyclic hardening with the difference of TS 43 MPa with surprisingly increased value 1.7 % of El. together with almost not changed CVN values. Achieved TS results in **Table 3** correspond with work of Portella and Rie [14] where the effect of cycle loading to AIS 4135 steel is clearly described however cyclic strengthening was even more intensive. **Figure 3** represents the crack initiation up to the final crack area and it is clearly distinguishable that the MSS shows primarily the transcrystalline cleavage fracture with minority of intercrystalline fracture, see **Figure 3(3),** presence in limited area that is attributed to the potential different fracture behaviour of interface between the present δ-ferrite and the basic tempered martensitic matrix. **Figure 4** shows the entire fracture surface of AISI 4135 steel based on the transcrystalline cleavage fracture in majority together with the ductile fracture corresponding with [10].

4. CONCLUSION

This presented paper clearly describes the resistance of two different steel types (MSS and AISI 4135) to the tri-axial cycle loading. It was clearly distinguished that that the MSS revealed the microstructure of tempered martensite with presence of δ-ferrite in portion 8 - 10 wt. % and undergoes the cyclic softening proved by the decrease of TS by 14 MPa and increase of El. by 5 % together with CVN values increase. Fracture surface Presence of limited small areas of intercrystalline fracture is going to be a point of future research to clearly distinguish the essence of this phenomenon.

The AISI 4135 steel showed significant cyclic hardening behaviour. The increase of TS was recorder on the level of 43 MPa however with an increase value of El. that increased from 16 % to 17.7 %. CVN values were not almost changed. There will be of future more extensive research and testing done to explore the origin of increasing El. values even though the TS is increasing. Fracture surface revealed mainly transcrystalline cleavage fracture typical for AISI 4135 steel as it is documented in [10].

This paper can be used as a background and supporting material for a constructors and designers of pressure components that are going to be tri-axially loaded to make calculations of components durability more accurate and safe.

ACKNOWLEDGEMENTS

This paper was created in company of VÍTKOVICE CYLINDERS Inc. and at the FMMI within the project No. LO1203 "Regional Materials Science and Technology Centre - Feasibility program" founded by Ministry of Education, Youth and Sports of Czech.

REFERENCES

[1] MESQUITA, T., J., CHAUVEAU, E., MANTEL, M., BOUVIER, N., KOSCHEL, D. Corrosion and metallurgical investigation of two supermartensitic stainless steels for oil and gas environments. *Corr. Sci.*, 2014, vol. 81, pp. 152 - 161.

[2] KUMAR, B.S., KAIN, V., SINGH, M., VISHWANADH, B. Influence of hydrogen on mechanical properties and fracture of tempered 13 w t% Cr martensitic stainless steel. *Mater. Sci. Eng. A*, 2017, vol. 700, pp. 140 - 151.

[3] MONNOT, M., NOGUEIRA, R.P., ROCHE, V., BERTHOMÉ, G., CHAUVEAU, E., ESTEVEZ, R., MANTEL, M. Sulfide stress corrosion study of a super martensitic stainless steel in H_2S sour environments: Metallic sulphides formation and hydrogen embrittlement. *Appl. Surf. Sci.*, 2017, vol. 394, pp. 132 - 141.

[4] SILVERSTEIN, R., ELIEZER, D. Mechanisms of hydrogen trapping in austenitic, duplex, and super martensitic stainless steels. J. *Alloys Comp.*, 2017, vol. 720, pp. 451 - 459.

[5] FOROOZMEHR, F., VERREMAN, Y., CHEN, J. THIBAULT, D., BOCHER, P. Effect of inclusions on fracture behaviour of cast and wrought 13% Cr-4% Ni martensitic stainless steels. *Eng. Frac. Mech.*, 2017, vol. 175, pp. 262 - 278.

[6] MA, X.P., WANG, L.J., SUBRAMANIAN, S.V., LIU, C.M., CHUNMING, L. Studies on Nb Microalloying of 13Cr Super Martensitic Stainless Steel. *Metall. Mat. Trans. A*, 2012, vol. 43, no. 12, pp. 140 - 151.

[7] MA, X.P., WANG, L.J., QIN, B., LIU, C.M., SUBRAMANIAN, S., V. Effect on F on microstructure and mechanical properties of 16Cr5Ni1Mo. *Materials Design*, 2012, vol. 34, pp. 74 - 81.

[8] YE, D., LI, J., JIANG, W., SU, J., ZHAO, K. Effect of Cu addition on microstructure and mechanical properties of 15 % Cr super martensitic stainless steel. *Materials Design*, 2012, vol. 41, pp. 16 - 22.

[9] MA, X.P., WANG, L.J., LIU, C.M., SUBRAMANIAN, S., V. Microstructure and properties of 13Cr5Ni1Mo0.025Nb0.09V0.06N super martensitic stainless steel. *Mat. Sci. Eng. A*, 2012, vol. 539, pp. 271 - 279.

[10] KUČERA, P. MAZANCOVÁ. E. Changes of Mechanical Properties in Response to Changes in Microstructure of High Pressure Steel Cylinders obtained by Various Heat Treatments. *Mater. Sci. Forum*, 2014, vol. 782, pp. 191 - 196.

[11] SCANDELLA, F., CAVALLIN, N., GRESSEL, P., HAOUAS, J., JUBIN, L., LEFEBVRE, F., HUTHER, I. Use of martensitic stainless steel welding consumable to substantially improve the fatigue strength of low alloy steel welded structures. *Procedia Engineering*, 2014, vol. 66, pp. 108 - 125.

[12] NIESSEN, F., TIEDJE, N.S., HALD, J. Kinetics modelling of delta-ferrite formation and retainment during casting of supermartensitic stainless steel. *Materials Design*, 2017, vol. 118, pp. 138 - 145.

[13] WANG, P., LU, S.P., XIAO, N.M., LI, D.ZD., LI, Y.Y. Effect of delta ferrite in impact properties of low carbon 13Cr-4Ni martensitic stainless steel. *Mat. Sci. Eng.*, 2010, vol. 527, pp. 3210 - 3216.

[14] PORTELLA, P.D., RIE, K.T. *Low Cycle Fatigue and Elasto-Plastic Behaviour of Materials. 1st ed.* Oxford: Elsevier Science, 1998. 890 p.